

Inclusive Search for the SM Higgs Boson in the $H \rightarrow \gamma\gamma$ channel at the LHC

Serguei Ganjour

CEA-Saclay/IRFU, F-91191 Gif-sur-Yvette, France
E-mail: Serguei.Ganjour@cea.fr

Abstract. A prospective for the inclusive search of the Standard Model Higgs boson in the decay channel $H \rightarrow \gamma\gamma$ is presented with the CMS experiment at the LHC. The analysis relies on a strategy to determine the background characteristics and systematics from data. The strategy is applied to a Monte Model of the QCD background, with full simulation of the detector response. The discrimination between signal and background exploits information on photon isolation and kinematics. The resolution for the reconstructed Higgs boson mass profits from the excellent energy resolution of the CMS crystal calorimeter. A discovery significance above 5 sigma is expected at integrated LHC luminosities below 30 fb^{-1} for Higgs boson masses below $140 \text{ GeV}/c^2$.

Keywords: LHC, CMS, Higgs

PACS: 14.80.Bn

INTRODUCTION

Since the beginning of the LHC project the $H \rightarrow \gamma\gamma$ channel is considered as a major discovery channel of Higgs particles [1] at masses between LEP limit $114.4 \text{ GeV}/c^2$ [2] and about $140 \text{ GeV}/c^2$. Indeed, despite a high rate of the $H \rightarrow b\bar{b}$ decays at low mass, it remains out of our interest due to large QCD background and low mass resolution of the di-jets state. Since the $H \rightarrow \gamma\gamma$ decay involves virtual loops, it has relatively small branching fraction of about 10^{-3} . However, the signal has a clean signature with two high E_T isolated photons. Due to an excellent resolution of the CMS electromagnetic calorimeter (ECAL), it can be identified as a narrow peak at a Higgs boson mass on the top of continuous background.

We investigated two analysis methods for the $H \rightarrow \gamma\gamma$ searches at CMS [3, 4]. In addition to the conventional cut based analysis, we report the optimized discovery oriented technique based on a multivariate optimization.

This study exploits a full CMS detector simulation program assuming $2 \times 10^{33} \text{ cm}^{-2} \text{ s}^{-1}$ machine luminosity and including collision effects such as minimum bias and underling events in the simulation model.

RATES AND CROSS SECTIONS

The inclusive search of the Higgs boson implies any production mechanism. In pp collisions at LHC energy about 80% of the Higgs bosons are produced in the gluon fusion reaction, while the rest are produced in association with either $q\bar{q}$ pairs (VWB or

$t\bar{t}$ fusion) or vector bosons. Table 1 presents the cross sections and $H \rightarrow \gamma\gamma$ branching ratios for the different Higgs boson mass [6].

TABLE 1. Signal NLO cross sections and branching ratios.

M_H (GeV/ c^2)	115	120	130	140	150
σ gg fusion (pb)	39.2	36.4	31.6	27.7	24.5
σ WVB fusion (pb)	4.7	4.5	4.1	3.8	3.6
σ WH, ZH, $t\bar{t}H$ (pb)	3.8	3.3	2.6	2.1	1.7
Total σ (pb)	47.6	44.2	38.3	33.6	29.7
$\mathcal{B}(H \rightarrow \gamma\gamma)$, %	0.21	0.22	0.22	0.20	0.14
$\sigma \times \mathcal{B}$ (fb)	99.3	97.5	86.0	65.5	41.5

We consider two sorts of the background processes. The “irreducible” background has two real high E_T isolated photons. Such a signature can be produced by both $q\bar{q}$ annihilation (“born”) and gg fusion (“box”) as well as qg Compton scattering with isolated bremsstrahlung processes. We estimate the total differential rate of “irreducible” backgrounds about 100 fb/GeV/ c^2 at 120 GeV/ c^2 mass. Thus, for a powerful discrimination of signal we require about 1 GeV/ c^2 two-photon mass resolution (see Table 1).

TABLE 2. LO cross sections for backgrounds.

Process	p_T (GeV/ c)	σ_{LO} (pb)
pp $\rightarrow \gamma\gamma$ (born)	> 25	82
pp $\rightarrow \gamma\gamma$ (box)	> 25	82
pp $\rightarrow \gamma$ +jet	> 30	5×10^4
pp \rightarrow jets	> 50	2.8×10^7
Drell Yan ee	–	4×10^3

Dominant QCD processes like γ +jet and di-jets may lead to the fake photons induced by neutral hadrons π^0 or η and produced in the jet fragmentation processes. The “reducible” background has at least one non-isolated photon. The PYTHIA LO cross sections of the background processes are presented in Table 2. The K-factors applied to compute the background yields at NLO cross sections are summarized in Table 3 [7]. Thus, a jet suppression has to be better than 10^{-3} to diminish its rate at the level of the “irreducible” background.

TABLE 3. Background K-factors applied for the PYTHIA cross section

Process	K-factor
pp $\rightarrow \gamma\gamma$ (born)	1.5
at the test-beam. pp $\rightarrow \gamma\gamma$ (box)	1.2
pp $\rightarrow \gamma$ +jet (2 prompt)	1.72
pp $\rightarrow \gamma$ +jet (1 prompt)	1
pp \rightarrow jets	1

DETECTOR

The conceptual design of the CMS detector exploits the conventional layout of the particle detector at hadron colliders [5]. A dedicated electromagnetic calorimeter is required for a powerful search of the Standard Model (SM) Higgs boson. Indeed, the $H \rightarrow \gamma\gamma$ decay was employed as a benchmark channel in the design of the ECAL. It comprises 75848 lead tungstate (PWO_4) crystals placed in two regions: the barrel ($|\eta| < 1.479$) and the endcap ($1.479 < |\eta| < 3.0$). The ECAL endcap is equipped by a preshower (ES) system for π^0 rejection. Due to low Moliere radius (2.19 cm) about 80% of the shower energy is deposited in one crystal having $2.2 \times 2.2 \text{ cm}^2$ front face size. Such a high granularity allows us a powerful identification of isolated photons.

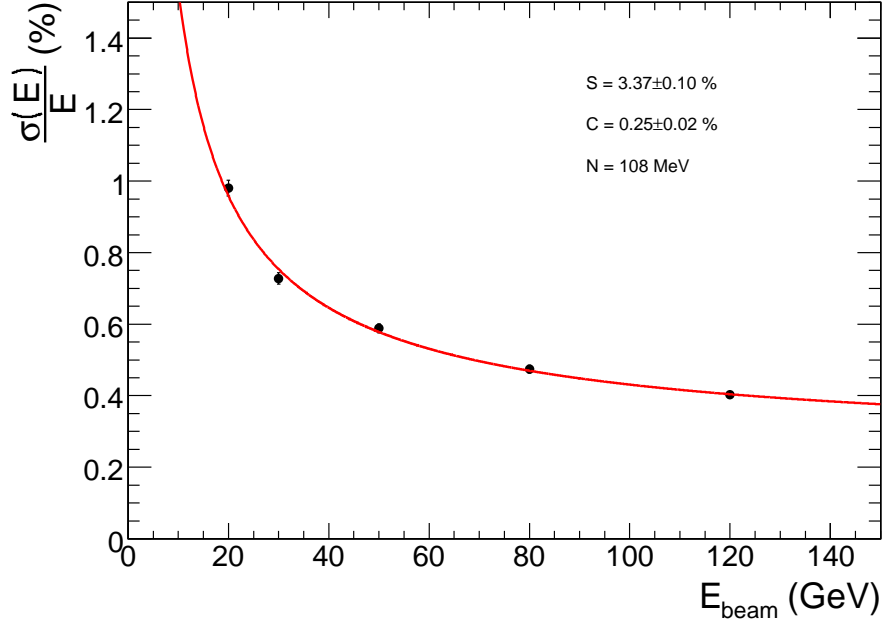


FIGURE 1. Energy resolution of the barrel supermodule.

Figure 1 shows the energy resolution of the ECAL barrel obtained with an electron test-beam. The stochastic (S), the noise (N) and the constant (C) terms are obtained by a fit with the following function:

$$\left(\frac{\sigma}{E}\right)^2 = \left(\frac{S}{\sqrt{E}}\right)^2 + \left(\frac{N}{E}\right)^2 + C^2. \quad (1)$$

Clustering algorithm accounts strong magnetic field and presence of material in front of the calorimeter. Measured energy can be computed as

$$E_{e,\gamma} = F \times \sum_{\text{clusters}} Gc_i A_i, \quad (2)$$

where F is a correction function, Gc_i is a calibration factor expressed as a product of a global absolute scale and intercalibration constants, respectively. A_i is a signal amplitude, in ADC counts. Sum of the incident energy in 5×5 crystals provide the best

energy estimation for the unconverted photons ($F = 1$). The dedicated procedure of ECAL calibration is foreseen with the physics event such as $W \rightarrow e\nu$, $Z \rightarrow e^+e^-$ and $\pi^0 \rightarrow \gamma\gamma$.

ANALYSIS AND RESULTS

Higgs decays into two-photon state are selected with extremely high efficiency both Level-1 (99.7%) and High Level Triggers (88.4%). Due to tighter kinematical and isolation criteria applied in the analysis, no additional signal restriction by trigger were observed.

Two photon candidates are selected within fiducial volume $|\eta| < 2.5$, and $p_T^\gamma > 40, 35$ GeV/c. Since fake photons produced in jets are accompanied by additional energetic particles, we require no tracks with $p_T > 1.5$ GeV/c inside a cone around photon with a radius $\Delta R < 0.3$. In addition, we demand $\sum E_T < 6(3)$ GeV/c in the ECAL barrel (endcap) in a cone $0.06 < \Delta R < 0.35$ and $\sum E_T < 6(5)$ GeV/c in the HCAL barrel (endcap) in a cone $\Delta R < 0.3$. The energy response of individual crystals were smeared according to calibration precision expected for an integrated luminosity of 10 fb^{-1} and obtained with $W \rightarrow e\nu$ events. Due to longitudinal spread of the interaction vertices (~ 50 mm) the di-photon mass is smeared by about $1.5 \text{ GeV}/c^2$. Indeed, Higgs bosons are produced in association with tracks from underlying events, initial state gluon radiation and associative particles qqH, WH, ZH . These tracks allow us to indentify the interaction vertex, in about 80% of cases, and correct momenta of the photons.

Figure 2 shows the di-photon mass distribution for the signal (scaled by a factor 10) and the background events after the selection. For a $120 \text{ GeV}/c^2$ Higgs boson, the signal efficiency of 30% yields to 29.3 observed Higgs events per inverse femtobarn, while the total background is $178 \text{ fb}/\text{GeV}/c^2$ as shown in Table 4. Despite asymmetric lineshape about 60% of the signal remains within $\pm 1 \text{ GeV}/c^2$ mass window.

TABLE 4. Background yields in $\text{fb}/\text{GeV}/c^2$

Process	$M_H, (\text{GeV}/c^2)$			
	115	120	130	140
$pp \rightarrow \gamma\gamma$ (born)	48	44	36	29
$pp \rightarrow \gamma\gamma$ (box)	36	31	23	16
$pp \rightarrow \gamma + \text{jet}$ (2prompt)	43	40	32	26
$pp \rightarrow \gamma + \text{jet}$ (1prompt)	40	34	22	19
$pp \rightarrow \text{jets}$	29	27	20	18
Drell Yan ee	2	2	1	1
Total background	203	178	134	109

New variables or cuts optimization do not lead to the further improvement of the signal over background ratio (s/b). However, we find the R_9 , fraction of the super-cluster energy deposited a small 3×3 crystal area, as a powerful discriminator of a π^0 . Indeed, high value of R_9 readily identifies converted photons and automatically selects against π^0 . The converted category remains background enriched. However, the use of a track information would allow further rejection of the background.

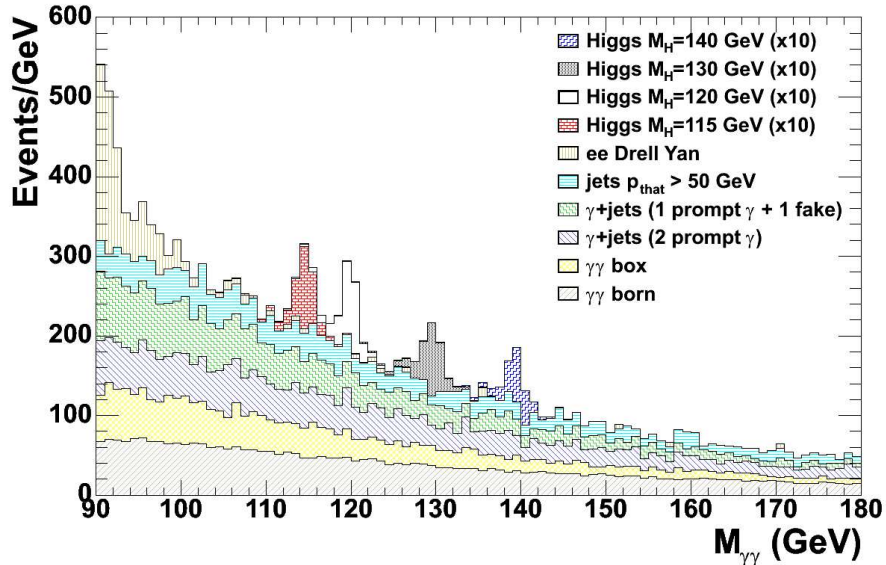


FIGURE 2. Expected di-photon invariant mass distribution for the cut-based analysis normalized to an integrated luminosity of 1 fb^{-1} . Signal is scaled by a factor 10.

To improve signal significance, we split the analyzed sample into categories with different s/b . Besides *single category*, we consider *four categories*, 2 categories where both photons are detected in the barrel and 2 where at least one photon is in the endcap. Each of these 2 categories are splitted for high (>0.93) and low (<0.93) values of R_9 . Then, we form *twelve categories* sample based on 3 ranges in R_9 (0.9, 0.948) and 4 pseudo-rapidity regions in $|\eta|$ (0.9, 1.4, 2.1). Table 5 summarizes the integrated luminosity needed to discover or to exclude Higgs boson for the different event splitting. Confidence levels are computed with a frequentistic approach using a log-likelihood ratio (LLR) estimator. These outcomes are computed for many possible pseudo-experiments for a hypothesis when the signal exists and that it does not.

TABLE 5. Integrated luminosity required for observation or exclusion of the Higgs boson with a mass of $120 \text{ GeV}/c^2$.

	5σ	3σ	95% C.L. excl.
1 category	24.5 (39.5)	8.9 (11.5)	4.1 (5.8)
4 categories	21.3 (26.0)	7.5 (9.1)	3.5 (4.8)
12 categories	19.3 (22.8)	7.0 (8.1)	3.2 (4.4)

The optimized analysis exploits six categories, 3 categories where both photons are detected in the barrel and 3 where at least one photon is in the endcap. These 3 categories are defined according to measured R_9 , as for the cut-based analysis splitted into 12 categories. Loose cuts are applied for the isolation variables which are used as a neural network prior. Fixed cut for the optimized NN_{iso} output variable slightly improves a background rejection. Besides two-photon mass four other kinematical variables can be used for further discrimination of the signal. They are transverse energy of each photon $E_T^{\gamma^{1,2}}$, η difference between two photons and longitudinal momentum of the

photon pair $P_L^{\gamma\gamma}$. These variables are combined with NN_{iso} for the further neural network optimization. To reject background the neural net is trained with the mass side-band events and results into NN_{kin} output variable. Due to negligible correlation between invariant mass and NN_{kin} , the s/b expectation can be estimated for each event as

$$\left(\frac{s}{b}\right)_{est} = \left(\frac{s}{b}\right)_{mass} \times \left(\frac{s}{b}\right)_{kin}. \quad (3)$$

Finally, the events are binned according to the s/b estimate. Then, we exploit $\log(s/b)$ distribution to compute the confidence level with the LLR estimator.

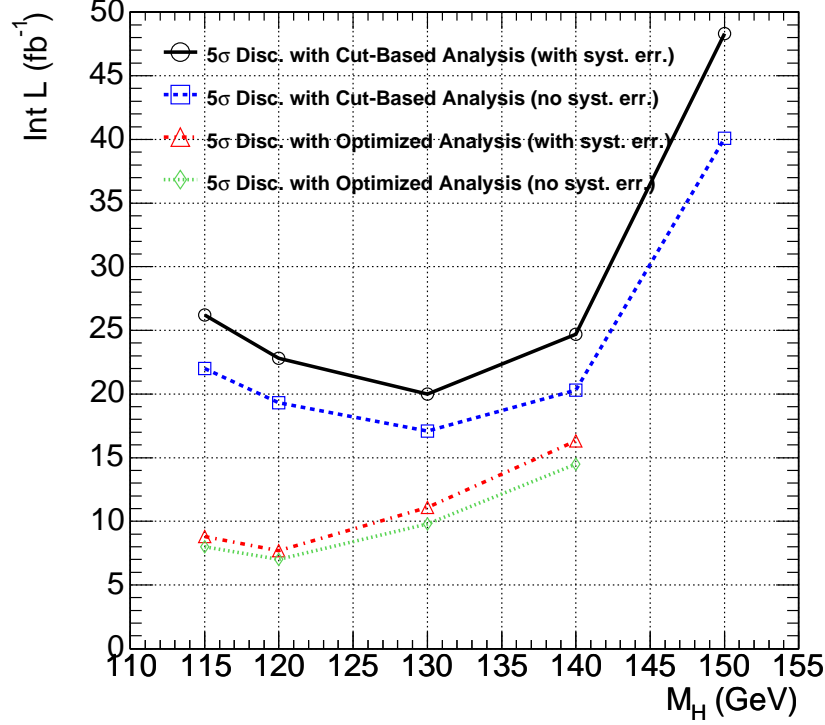


FIGURE 3. Integrated luminosity required for a 5σ discovery as a function of the Higgs mass.

Figure 3 shows the integrated luminosity needed for a 5σ discovery. For a $120 \text{ GeV}/c^2$ Higgs boson, such a discovery can occur with about 7.7 fb^{-1} recorded data using an optimized technique, while it is required about 22.8 fb^{-1} of integrated luminosity using conventional cut-based analysis technique (see Table 5). We address major systematic errors. The dominant contribution is due to background subtraction. It is evaluated from the uncertainty of the fit function in the mass side-bands.

CONCLUSIONS

The SM Higgs boson can be readily discovered with an integrated luminosity less than 30 fb^{-1} , if its mass is below $140 \text{ GeV}/c^2$. We investigated the standard cut-based and discovery oriented optimized analysis techniques. The best achievement corresponds to

a 120 GeV/c² Higgs boson where 7.7 fb⁻¹ is required for the 5 σ discovery. The analysis strategy implies data driven methods of the background subtraction using a side-band mass regions. There is a potential room for improvement by adding the track information to identify converted photons and ECAL preshower to reject π^0 .

REFERENCES

1. CMS Collaboration, "The Compact Muon Solenoid Technical Proposal", *CERN/LHCC* 1994-38
2. LEP Working Group for Higgs Boson Searches Collaboration, R. Barate *et al*, *Phys.Lett.* **B 565** 61
3. CMS Collaboration, "The CMS Physics Technical Design Report, Volume II", *CERN/LHCC*, 2006-021
4. CMS Collaboration, M. Pieri *et al*, *CMS-NOTE-2006/112*
5. CMS Collaboration, "The CMS Physics Technical Design Report, Volume I", *CERN/LHCC*, 2006-001
6. M. Spira, *arXiv*: hep-ph/9510347; A. Djouadi, J. Kalinowski and M. Spira, *Comput.Phys.Commun.* **108** (1998), 56 (*arXiv*: hep-ph/9704448)
7. T. Binoth *et al*, *arXiv*: hep-ph/0005194; T. Binoth *et al*, *arXiv*: hep-ph/0204316; T. Binoth *et al*, *arXiv*: hep-ph/0203064; T. Binoth *et al*, *arXiv*: hep-ph/0403100; Z. Bern *et al*, *Phys.Rev.* **D 66** 074018 (2002)